
ELSEVIER

Journal of Computational and Applied Mathematics 149 (2002) 71–82

JOURNAL OF COMPUTATIONAL AND APPLIED MATHEMATICS

www.elsevier.com/locate/cam

Direct simulation of the motion of a settling ellipsoid in Newtonian fluid

Tsorng-Whay Pan[a], Roland Glowinski[a,*], Giovanni P. Galdi[b]

[a] *Department of Mathematics, University of Houston, Houston, 4800 Calhouwd Road, 77204 Houston, TX, USA*
[b] *Department of Mechanical Engineering, University of Pittsburg, Pittsburg, PA 15261, USA*

Received 24 October 2001; received in revised form 18 December 2001

Abstract

In this paper, we discuss the generalization of a Lagrange multiplier-based fictitious domain method to the simulation of the motion of general shape particles in Newtonian fluid. Preliminary numerical results of a settling ellipsoid in a narrow channel filled with a Newtonian fluid are presented. As expected, the ellipsoid turns its broadside to the stream in the simulations.

1. Introduction

The orientation of symmetric long body (loosely, a long body is a body where one dimension is much prevailing upon the other two) in liquids of different nature is a fundamental issue in many problems of practical interest (see [15], and references therein). In this article we first discuss the generalization of a Lagrange multiplier based fictitious domain method [8,10] to the simulation of the motion of particles of general shape in a Newtonian fluid. Unlike the cases where the particles are spheres, we attach two points to each particle of general shape and move them according to the rigid-body motion of the particle in order to track the motion of the particle. The equations describing the motion of these two points are solved by a distance preserving scheme so that rigidity can be maintained. We then apply it to simulate the settling of an ellipsoid in a narrow channel filled with a Newtonian fluid. In the simulation, the ellipsoid turns its broadside to the stream as expected. Preliminary numerical results are presented.

* Corresponding author.
E-mail address: roland@math.uh.edu (R. Glowinski).

0377-0427/02/$ - see front matter
PII: S0377-0427(02)00521-6

2. A model problem and fictitious domain formulation for three-dimensional particulate flow

To perform the *direct numerical simulation* of the interaction between particles and fluid, we have developed a methodology which is a combination of a distributed Lagrange multiplier-based fictitious domain (also called domain embedding) method and operator splitting methods [6–10], this approach (or closely related ones derived from it) has become the method of choice for other investigators around the world (Refs., [2,23]). We are going to recall the ideas at the basis of the above methodology by considering the motion of a single particle in a Newtonian viscous incompressible fluid (of density ρ_f and viscosity ν_f) under the effect of gravity; actually, the generalization to a thousand of spherical particles in 3D and 10 000 circular particles in 2D is possible as shown in [10,18,19]. For the situation depicted in Fig. 1 (for nonspherical particle cases), the flow is modeled by the Navier–Stokes equations, namely, (with obvious notation)

$$\rho_f \left[\frac{\partial \mathbf{u}}{\partial t} + (\mathbf{u} \cdot \boldsymbol{\nabla})\mathbf{u} \right] - \nu_f \Delta \mathbf{u} + \boldsymbol{\nabla} p = \rho_f \mathbf{g} \quad \text{in } \Omega \backslash \bar{B}(t), (0, T), \tag{1}$$

$$\boldsymbol{\nabla} \cdot \mathbf{u} = 0 \quad \text{in } \Omega \backslash \bar{B}(t), (0, T), \tag{2}$$

$$\mathbf{u}(0) = \mathbf{u}_0(\mathbf{x}) \quad (\text{with } \boldsymbol{\nabla} \cdot \mathbf{u}_0 = 0), \tag{3}$$

$$\mathbf{u} = \mathbf{g}_0 \quad \text{on } \Gamma \times (0, T) \quad \text{with } \int_\Gamma \mathbf{g}_0 \cdot \mathbf{n} \, \mathrm{d}\Gamma = 0; \tag{4}$$

where $\Gamma = \partial\Omega$, $\mathbf{g}$ is gravity and $\mathbf{n}$ is the unit normal vector pointing outward to the flow region. We assume a *no-slip condition* on $\gamma(=\partial B)$. The motion of particle B satisfies the Euler–Newton's equations, namely

$$\mathbf{v}(\mathbf{x}, t) = \mathbf{V}(t) + \overrightarrow{\boldsymbol{\omega}}(t) \times \overrightarrow{\mathbf{G}(t)\mathbf{x}} \quad \forall \{\mathbf{x}, t\} \in \bar{B}(t) \times (0, T), \tag{5}$$

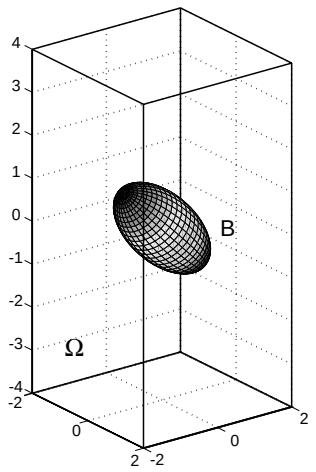

Fig. 1. The flow region with one particle.

$$\frac{\mathrm{d}\mathbf{G}}{\mathrm{d}t} = \mathbf{V}, \tag{6}$$

$$M_\mathrm{p}\frac{\mathrm{d}\mathbf{V}}{\mathrm{d}t} = M_\mathrm{p}\mathbf{g} + \mathbf{F}_\mathrm{H} + \mathbf{F}^r, \tag{7}$$

$$\frac{\mathrm{d}(\mathbf{I}_\mathrm{p}\boldsymbol{\omega})}{\mathrm{d}t} = \mathbf{T}_\mathrm{H} + \overrightarrow{\mathbf{G}\mathbf{x}_r} \times \mathbf{F}^r \tag{8}$$

with hydrodynamical forces and torques

$$\mathbf{F}_\mathrm{H} = -\int_\gamma \boldsymbol{\sigma}\mathbf{n}\,\mathrm{d}\gamma, \quad \mathbf{T}_\mathrm{H} = -\left(\int_\gamma \overrightarrow{\mathbf{G}\mathbf{x}} \times \boldsymbol{\sigma}\mathbf{n}\,\mathrm{d}\gamma\right), \tag{9}$$

completed by the following initial conditions:

$$\mathbf{G}(0) = \mathbf{G}_0, \quad \mathbf{V}(0) = \mathbf{V}_0, \quad \boldsymbol{\omega}(0) = \boldsymbol{\omega}_0. \tag{10}$$

Above, M_p, $\mathbf{I}_\mathrm{p}$, $\mathbf{G}$, $\mathbf{V}$ and $\boldsymbol{\omega}$ are the mass, inertia, center of mass, velocity of the center of mass and angular velocity of particle B, respectively. In (8) we found preferable to deal with the *kinematic angular momentum* $\mathbf{I}_\mathrm{p}\boldsymbol{\omega}$ making the formulation more conservative. In order to avoid particle–particle and particle–wall penetration which can happen in the numerical simulation, we have introduced a artificial force $\mathbf{F}^r$ in (7) (for more details, see, e.g., [8] and [10]) and then a torque in (8) acting on the point $\mathbf{x}_r$ where $\mathbf{F}^r$ applies on B.

To solve system (1)–(10) we can use, for example, *Arbitrary Lagrange–Euler* (ALE) methods as in [12,14,17], or *fictitious domain methods*, which allow the flow calculation on a fixed grid, as in [6–10]. The fictitious domain methods that we advocate have some common features with the *immersed boundary method* of Ch. Peskin (see, e.g., Refs. [20–22]) but also some significant differences in the sense that we take systematically advantage of *distributed Lagrange multipliers* to force the rigid-body motion inside the particle, which seems still to be a relatively novel approach in this context, and whose possibilities have not been fully explored yet. As with the methods in [20–22], our approach takes advantage of the fact that the flow can be computed on a grid which does not have to vary in time, a substantial simplification indeed.

The principle of fictitious domain methods is simple. It consists of

- Filling the particle with a fluid having the same density and viscosity as the surrounding one.
- Compensating the above step by introducing, in some sense, an *anti-particle* of mass $(-1)M_\mathrm{p}\rho_\mathrm{f}/\rho_\mathrm{s}$ and inertia $(-1)\mathbf{I}_\mathrm{p}\rho_\mathrm{f}/\rho_\mathrm{s}$, taking into account the fact that any rigid-body motion $\mathbf{v}(\mathbf{x},t)$ verifies $\boldsymbol{\nabla}\cdot\mathbf{v} = 0$ and $\mathbf{D}(\mathbf{v}) = \mathbf{0}$ (ρ_s: particle density).
- Finally, imposing the rigid-body velocity on $\bar{B}(t)$, namely

$$\mathbf{v}(\mathbf{x},t) = \mathbf{V}(t) + \vec{\boldsymbol{\omega}}(t) \times \overrightarrow{\mathbf{G}(t)\mathbf{x}} \quad \forall \mathbf{x} \in \bar{B}(t) \ \ \forall t \in (0,T), \tag{11}$$

  via a Lagrange multiplier $\boldsymbol{\lambda}$ supported by $\bar{B}(t)$. Vector $\boldsymbol{\lambda}$ forces rigidity in $B(t)$ in the same way that $\boldsymbol{\nabla}p$ forces $\boldsymbol{\nabla}\cdot\mathbf{v} = 0$ for incompressible fluids.

We obtain then an equivalent formulation of (1)–(10) defined on the whole domain, namely
For a.e. $t > 0$, find $\{\mathbf{u}(t), p(t), \mathbf{V}(t), \mathbf{G}(t), \boldsymbol{\omega}(t), \boldsymbol{\lambda}(t)\}$

such that

$$\mathbf{u}(t)\in\mathbf{W}_{\mathbf{g}_0}(t),\ p(t)\in L^2_0(\Omega),\ \mathbf{V}(t)\in\mathbb{R}^3,\ \mathbf{G}(t)\in\mathbb{R}^3,\boldsymbol{\omega}(t)\in\mathbb{R}^3,\ \boldsymbol{\lambda}(t)\in\Lambda(t) \tag{12}$$

and

$$\begin{aligned}
&\rho_{\mathrm{f}}\int_\Omega\left[\frac{\partial\mathbf{u}}{\partial t}+(\mathbf{u}\cdot\boldsymbol{\nabla})\mathbf{u}\right]\cdot\mathbf{v}\,\mathrm{d}\mathbf{x}-\int_\Omega p\boldsymbol{\nabla}\cdot\mathbf{v}\,\mathrm{d}\mathbf{x}\\
&+\nu_{\mathrm{f}}\int_\Omega\boldsymbol{\nabla}\mathbf{u}:\boldsymbol{\nabla}\mathbf{v}\,\mathrm{d}\mathbf{x}-\langle\boldsymbol{\lambda},\mathbf{v}-\mathbf{Y}-\boldsymbol{\theta}\times\mathbf{G}\mathbf{x}\rangle_{\Lambda(t)}\\
&+\left(1-\frac{\rho_{\mathrm{f}}}{\rho_{\mathrm{s}}}\right)\left[M_{\mathrm{p}}\frac{\mathrm{d}\mathbf{V}}{\mathrm{d}t}\cdot\mathbf{Y}+\frac{\mathrm{d}(\mathbf{I}_{\mathrm{p}}\boldsymbol{\omega})}{\mathrm{d}t}\cdot\boldsymbol{\theta}\right]-\mathbf{F}^r\cdot\mathbf{Y}-\overrightarrow{\mathbf{G}\mathbf{x}_r}\times\mathbf{F}^r\cdot\boldsymbol{\theta}\\
&\quad=\left(1-\frac{\rho_{\mathrm{f}}}{\rho_{\mathrm{s}}}\right)M_{\mathrm{p}}\mathbf{g}\cdot\mathbf{Y}+\rho_{\mathrm{f}}\int_\Omega\mathbf{g}\cdot\mathbf{v}\,\mathrm{d}\mathbf{x}\quad\forall\mathbf{v}\in(H^1_0(\Omega))^3,\ \forall\mathbf{Y}\in\mathbb{R}^3\ ,\forall\boldsymbol{\theta}\in\mathbb{R}^3,
\end{aligned}\tag{13}$$

$$\int_\Omega q\boldsymbol{\nabla}\cdot\mathbf{u}(t)\,\mathrm{d}\mathbf{x}=0\quad\forall q\in L^2(\Omega), \tag{14}$$

$$\frac{\mathrm{d}\mathbf{G}}{\mathrm{d}t}=\mathbf{V}, \tag{15}$$

$$\langle\boldsymbol{\mu},\mathbf{u}(t)-\mathbf{V}(t)-\boldsymbol{\omega}(t)\times\mathbf{G}(t)\mathbf{x}\rangle_{\Lambda(t)}=0\quad\forall\boldsymbol{\mu}\in\Lambda(t), \tag{16}$$

$$\mathbf{V}(0)=\mathbf{V}_0,\quad\boldsymbol{\omega}(0)=\boldsymbol{\omega}_0,\quad\mathbf{G}(0)=\mathbf{G}_0, \tag{17}$$

$$\mathbf{u}(\mathbf{x},0)=\tilde{\mathbf{u}}_0(\mathbf{x})=\begin{cases}\mathbf{u}_0(\mathbf{x}) & \forall\mathbf{x}\in\Omega\backslash\overline{B(0)},\\ \mathbf{V}_0+\boldsymbol{\omega}_0\times\mathbf{G}_0\mathbf{x} & \forall\mathbf{x}\in\overline{B(0)}\end{cases} \tag{18}$$

with the following functional spaces:

$$\mathbf{W}_{\mathbf{g}_0}(t)=\left\{\mathbf{v}\,|\,\mathbf{v}\in(H^1(\Omega))^3,\mathbf{v}=\mathbf{g}_0(t)\text{ on }\Gamma\right\},$$

$$L^2_0(\Omega)=\left\{q\,\middle|\,q\in L^2(\Omega),\ \int_\Omega q\,\mathrm{d}\mathbf{x}=0\right\},\quad\Lambda(t)=(H^1(B(t)))^3.$$

In (12)–(18), only the center of mass, the translation velocity of the center of mass and the angular velocity of the particle are considered. Knowing these two velocities and the center of mass of the particle, one is able to translate and rotate the particle in space by tracking two extra points $\mathbf{x}_1$ and $\mathbf{x}_2$ in each particle, which follow the rigid-body motion:

$$\frac{\mathrm{d}\mathbf{x}_i}{\mathrm{d}t}=\mathbf{V}(t)+\overrightarrow{\boldsymbol{\omega}}(t)\times\overrightarrow{\mathbf{G}(t)\mathbf{x}_i},\quad\mathbf{x}_i(0)=\mathbf{x}_{i,0},\ \ i=1,2. \tag{19}$$

In practice we shall track two orthogonal normalized vectors rigidly attached to the body B and originating from the center of mass $\mathbf{G}$.

3. Time and space discretization

For simplicity, we assume that $\Omega \subset \mathbb{R}^3$ and is a rectangular parallelepiped. Concerning the *space approximation* of problem (12)–(19) by a *finite element method*, we have

$$\mathbf{W}_h = \{\mathbf{v}_h \,|\, \mathbf{v}_h \in (C^0(\bar{\Omega}))^3, \mathbf{v}_h|_T \in (P_1)^3 \quad \forall T \in \mathscr{T}_h\}, \tag{20}$$

$$\mathbf{W}_{0h} = \{\mathbf{v}_h \,|\, \mathbf{v}_h \in \mathbf{W}_h,\ \mathbf{v}_h = \mathbf{0} \text{ on } \Gamma\}, \tag{21}$$

$$L_h^2 = \{q_h \,|\, q_h \in C^0(\bar{\Omega}),\ q_h|_T \in P_1 \quad \forall T \in \mathscr{T}_{2h}\}, \quad L_{0h}^2 = \left\{q_h \,|\, q_h \in L_h^2, \int_\Omega q_h \,\mathrm{d}\mathbf{x} = 0\right\}, \tag{22}$$

where $\mathscr{T}_h$ is a tetrahedrization of Ω, $\mathscr{T}_{2h}$ is twice coarser than $\mathscr{T}_h$, and P_1 is the space of the polynomials in three variables of degree $\leqslant 1$. A finite-dimensional space approximating $\Lambda(t)$ is as follows: let $\{\boldsymbol{\xi}_i\}_{i=1}^N$ be a set of points form $\overline{B(t)}$ which cover $\overline{B(t)}$ (uniformly, for example); we define then

$$\Lambda_h(t) = \left\{\boldsymbol{\mu}_h \,|\, \boldsymbol{\mu}_h = \sum_{i=1}^N \boldsymbol{\mu}_i \delta(\mathbf{x} - \boldsymbol{\xi}_i),\ \boldsymbol{\mu}_i \in \mathbb{R}^3,\ \forall i = 1, \ldots, N\right\}, \tag{23}$$

where $\delta(\cdot)$ is the Dirac measure at $\mathbf{x} = \mathbf{0}$. Then we shall use $\langle \cdot, \cdot \rangle_h$ defined by

$$\langle \boldsymbol{\mu}_h, \mathbf{v}_h \rangle_h = \sum_{i=1}^N \boldsymbol{\mu}_i \cdot \mathbf{v}_h(\boldsymbol{\xi}_i) \quad \forall \boldsymbol{\mu}_h \text{ in } \Lambda_h(t),\ \mathbf{v}_h \in \mathbf{W}_h. \tag{24}$$

A typical choice of points for defining (23) is a collection of grid points for velocity field covered by the interior of the particle $B(t)$ and selected points from the boundary of $B(t)$.

Using the above finite-dimensional spaces leads to the following approximation for problem (12)–(19):

For a.e. $t > 0$, find $\{\mathbf{u}_h(t), p_h(t), \mathbf{V}(t), \mathbf{G}(t), \boldsymbol{\omega}(t), \boldsymbol{\lambda}_h(t)\}$ such that

$$\mathbf{u}(t) \in \mathbf{W}_h(t),\ p_h(t) \in L_{0h}^2(\Omega),\ \mathbf{V}(t) \in \mathbb{R}^3, \mathbf{G}(t) \in \mathbb{R}^3, \boldsymbol{\omega}(t) \in \mathbb{R}^3, \boldsymbol{\lambda}_h(t) \in \Lambda_h(t) \tag{25}$$

and

$$\begin{aligned}
&\rho_\mathrm{f} \int_\Omega \left[\frac{\partial \mathbf{u}_h}{\partial t} + (\mathbf{u}_h \cdot \boldsymbol{\nabla})\mathbf{u}_h\right] \cdot \mathbf{v} \,\mathrm{d}\mathbf{x} - \int_\Omega p_h \boldsymbol{\nabla} \cdot \mathbf{v} \,\mathrm{d}\mathbf{x} \\
&\quad + \nu_\mathrm{f} \int_\Omega \boldsymbol{\nabla}\mathbf{u}_h : \boldsymbol{\nabla}\mathbf{v} \,\mathrm{d}\mathbf{x} - \langle \boldsymbol{\lambda}_h, \mathbf{v} - \mathbf{Y} - \boldsymbol{\theta} \times \mathbf{G}\mathbf{x} \rangle_h \\
&\quad + \left(1 - \frac{\rho_\mathrm{f}}{\rho_\mathrm{s}}\right)\left[M_\mathrm{p} \frac{\mathrm{d}\mathbf{V}}{\mathrm{d}t} \cdot \mathbf{Y} + \frac{\mathrm{d}(\mathbf{I}_\mathrm{p}\boldsymbol{\omega})}{\mathrm{d}t} \cdot \boldsymbol{\theta}\right] - \mathbf{F}^r \cdot \mathbf{Y} - \overrightarrow{\mathbf{G}\mathbf{x}_r} \times \mathbf{F}^r \cdot \boldsymbol{\theta} \\
&= \left(1 - \frac{\rho_\mathrm{f}}{\rho_\mathrm{s}}\right) M_\mathrm{p} \mathbf{g} \cdot \mathbf{Y} + \rho_\mathrm{f} \int_\Omega \mathbf{g} \cdot \mathbf{v} \,\mathrm{d}\mathbf{x} \quad \forall \mathbf{v} \in \mathbf{W}_{0h},\ \forall \mathbf{Y} \in \mathbb{R}^3,\ \forall \boldsymbol{\theta} \in \mathbb{R}^3,
\end{aligned} \tag{26}$$

$$\int_\Omega q \boldsymbol{\nabla} \cdot \mathbf{u}_h(t) \,\mathrm{d}\mathbf{x} = 0 \quad \forall q \in L_h^2, \tag{27}$$

$$\mathbf{u}_h = \mathbf{g}_{0h} \quad \text{on } \Gamma, \tag{28}$$

$$\frac{\mathrm{d}\mathbf{G}}{\mathrm{d}t} = \mathbf{V}, \tag{29}$$

$$\frac{\mathrm{d}\mathbf{x}_i}{\mathrm{d}t} = \mathbf{V}(t) + \vec{\boldsymbol{\omega}}(t) \times \overrightarrow{\mathbf{G}(t)\mathbf{x}_i}, \quad \mathbf{x}_i(0) = \mathbf{x}_{i,0}, \quad i = 1, 2, \tag{30}$$

$$\langle \boldsymbol{\mu}, \mathbf{u}_h(t) - \mathbf{V}(t) - \boldsymbol{\omega}(t) \times \mathbf{G}(t)\mathbf{x} \rangle_h = 0 \quad \forall \boldsymbol{\mu} \in \Lambda(t), \tag{31}$$

$$\mathbf{V}(0) = \mathbf{V}_0, \quad \boldsymbol{\omega}(0) = \boldsymbol{\omega}_0, \quad \mathbf{G}(0) = \mathbf{G}_0, \tag{32}$$

$$\mathbf{u}(\mathbf{x}, 0) = \tilde{\mathbf{u}}_{0h}(\mathbf{x}). \tag{33}$$

In (28), $\mathbf{g}_{0h}$ is an approximation of $\mathbf{g}_0$ belonging to $\gamma\mathbf{W}_h = \{\mathbf{z}_h \mid \mathbf{z}_h \in (C^0(\Gamma))^3,\ \mathbf{z}_h = \tilde{\mathbf{z}}_h|_\Gamma \text{ with } \tilde{\mathbf{z}}_h \in \mathbf{W}_h\}$ and verifying $\int_\Gamma \mathbf{g}_{0h} \cdot \mathbf{n}\, \mathrm{d}\Gamma = 0$.

3.1. An operator-splitting scheme à la Marchuk–Yanenko

Many operator-splitting schemes can be used to time-discretize (25)–(33). One of the advantage of operator-splitting schemes is that we can decouple difficulties like (i) the incompressibility condition, (ii) the nonlinear advection term, and (iii) a rigid-body motion projection, so that each one of them can be handled separately, and in principle optimally. Let Δt be a time discretization step and $t^{n+s} = (n + s)\Delta t$. By an operator-splitting scheme à la Marchuk–Yanenko in [16], we have the following scheme after dropping some of the subscripts h (similar ones are discussed in [6–10]):

$$\mathbf{u}^0 = \tilde{\mathbf{u}}_0, \quad \mathbf{G}^0 = \mathbf{G}_0, \quad \mathbf{V}^0 = \mathbf{V}_0, \quad \boldsymbol{\omega}^0 = \boldsymbol{\omega}_0, \quad \mathbf{x}_1^0 = \mathbf{x}_{1,0}, \quad \mathbf{x}_2^0 = \mathbf{x}_{2,0} \quad \text{given;} \tag{34}$$

for $n \geqslant 0$, $\mathbf{u}^n (\simeq \mathbf{u}(t^n))$, $\mathbf{G}^n$, $\mathbf{V}^n$, $\boldsymbol{\omega}^n$, $\mathbf{x}_1^n$ and $\mathbf{x}_2^n$ being known, we compute $\mathbf{u}^{n+1/5}$, $p^{n+1/5}$ via the solution of

$$\begin{aligned}
&\rho_{\mathrm{f}} \int_\Omega \frac{\mathbf{u}^{n+1/5} - \mathbf{u}^n}{\Delta t} \cdot \mathbf{v}\, \mathrm{d}\mathbf{x} - \int_\Omega \mathbf{p}^{n+1/5} \boldsymbol{\nabla} \cdot \mathbf{v}\, \mathrm{d}\mathbf{x} = 0 \quad \forall \mathbf{v} \in \mathbf{W}_{0h}, \\
&\int_\Omega q \boldsymbol{\nabla} \cdot \mathbf{u}^{n+1/5}\, \mathrm{d}\mathbf{x} = 0 \quad \forall q \in L_h^2, \\
&\mathbf{u}^{n+1/5} \in \mathbf{W}_h, \quad \mathbf{u}^{n+1/5} = \mathbf{g}_{0h}^{n+1} \quad \text{on } \Gamma, \quad p^{n+1/5} \in L_{0h}^2.
\end{aligned} \tag{35}$$

Next, compute $\mathbf{u}^{n+2/5}$ via the solution of

$$\begin{aligned}
&\int_\Omega \frac{\partial \mathbf{u}}{\partial t} \cdot \mathbf{v}\, \mathrm{d}\mathbf{x} + \int_\Omega (\mathbf{u}^{n+1/5} \cdot \boldsymbol{\nabla})\mathbf{u} \cdot \mathbf{v}\, \mathrm{d}\mathbf{x} = 0 \quad \forall \mathbf{v} \in \mathbf{W}_{0h}^{n+1,-}, \quad \text{a.e. on } (t^n, t^{n+1}), \\
&\mathbf{u}(t^n) = \mathbf{u}^{n+1/5}, \\
&\mathbf{u}(t) \in \mathbf{W}_h, \quad \mathbf{u}(t) = \mathbf{g}_{0h}^{n+1} \quad \text{on } \boldsymbol{\Gamma}_-^{n+1} \times (t^n, t^{n+1}), \\
&\text{and set } \mathbf{u}^{n+2/5} = \mathbf{u}(t^{n+1}).
\end{aligned} \tag{36}$$

Then, compute $\mathbf{u}^{n+3/5}$ via the solution of

$$\rho_{\mathrm{f}} \int_{\Omega} \frac{\mathbf{u}^{n+3/5} - \mathbf{u}^{n+2/5}}{\Delta t} \cdot \mathbf{v}\, \mathrm{d}\mathbf{x} + \alpha \nu_{\mathrm{f}} \int_{\Omega} \nabla \mathbf{u}^{n+3/5} : \nabla \mathbf{v}\, \mathrm{d}\mathbf{x} = \rho_{\mathrm{f}} \int_{\Omega} \mathbf{g} \cdot \mathbf{v}\, \mathrm{d}\mathbf{x}$$

$$\forall \mathbf{v} \in \mathbf{W}_{0h};\ \ \mathbf{u}^{n+3/5} \in \mathbf{W}_h, \quad \mathbf{u}^{n+3/5} = \mathbf{g}_{0h}^{n+1} \quad \text{on } \Gamma. \tag{37}$$

Now predict the motion of the center of mass and the angular velocity of the particle via

$$\frac{\mathrm{d}\mathbf{G}}{\mathrm{d}t} = \mathbf{V}(t), \tag{38}$$

$$\frac{\mathrm{d}\mathbf{x}_i}{\mathrm{d}t} = \mathbf{V}(t) + \overrightarrow{\boldsymbol{\omega}}(t) \times \overrightarrow{\mathbf{G}(t)\mathbf{x}_i}, \quad \text{for } i = 1, 2, \tag{39}$$

$$(1 - \rho_{\mathrm{f}}/\rho_{\mathrm{s}})\, M_{\mathrm{p}} \frac{\mathrm{d}\mathbf{V}}{\mathrm{d}t} = (1 - \rho_{\mathrm{f}}/\rho_{\mathrm{s}})\, M_{\mathrm{p}} \mathbf{g} + \mathbf{F}^{r}, \tag{40}$$

$$(1 - \rho_{\mathrm{f}}/\rho_{\mathrm{s}})\, \frac{\mathrm{d}(\mathbf{I}_{\mathrm{p}}\boldsymbol{\omega})}{\mathrm{d}t} = \overrightarrow{\mathbf{G}\mathbf{x}_r} \times \mathbf{F}^{r}, \tag{41}$$

$$\mathbf{G}(t^n) = \mathbf{G}^n, \quad \mathbf{V}(t^n) = \mathbf{V}^n, \quad (\mathbf{I}_{\mathrm{p}}\boldsymbol{\omega})^n = (\mathbf{I}_{\mathrm{p}}\boldsymbol{\omega})(t^n), \quad \mathbf{x}_1(t^n) = \mathbf{x}_1^n, \quad \mathbf{x}_2(t^n) = \mathbf{x}_2^n, \tag{42}$$

for $t^n < t < t^{n+1}$. Then set $\mathbf{G}^{n+4/5} = \mathbf{G}(t^{n+1})$, $\mathbf{V}^{n+4/5} = \mathbf{V}(t^{n+1})$, $(\mathbf{I}_{\mathrm{p}}\boldsymbol{\omega})^{n+4/5} = (\mathbf{I}_{\mathrm{p}}\boldsymbol{\omega})(t^{n+1})$, $\mathbf{x}_1^{n+4/5} = \mathbf{x}_1(t^{n+1})$, and $\mathbf{x}_2^{n+4/5} = \mathbf{x}_2(t^{n+1})$.

With the center $\mathbf{G}^{n+4/5}$, $\mathbf{x}_1^{n+4/5}$ and $\mathbf{x}_2^{n+4/5}$ obtained at the above step, we enforce the rigid-body motion in the region $B(t^{n+4/5})$ occupied by the particle

$$\rho_{\mathrm{f}} \int_{\Omega} \frac{\mathbf{u}^{n+1} - \mathbf{u}^{n+4/5}}{\Delta t} \cdot \mathbf{v}\ d\boldsymbol{x} + \beta \nu_{\mathrm{f}} \int_{\Omega} \nabla \mathbf{u}^{n+1} : \nabla \mathbf{v}\, \mathrm{d}\mathbf{x}$$

$$+ (1 - \rho_{\mathrm{f}}/\rho_{\mathrm{s}}) M_{\mathrm{p}} \frac{\mathbf{V}^{n+1} - \mathbf{V}^{n+4/5}}{\Delta t} \cdot \mathbf{Y} + (1 - \rho_{\mathrm{f}}/\rho_{\mathrm{s}}) \frac{(\mathbf{I}_{\mathrm{p}}\boldsymbol{\omega})^{n+1} - (\mathbf{I}_{\mathrm{p}}\boldsymbol{\omega})^{n+4/5}}{\Delta t} \cdot \boldsymbol{\theta}$$

$$= \langle \boldsymbol{\lambda}^{n+4/5},\ \mathbf{v} - \mathbf{Y} - \boldsymbol{\theta} \times \overrightarrow{\mathbf{G}^{n+4/5}\mathbf{x}} \rangle_h \quad \forall \mathbf{v} \in \mathbf{W}_{0h},\ \ \mathbf{Y} \in \mathbb{R}^3,\ \ \boldsymbol{\theta} \in \mathbb{R}^3,$$

$$\mathbf{u}^{n+1} \in \mathbf{W}_h, \quad \mathbf{u}^{n+1} = \mathbf{g}_{0h}^{n+1} \quad \text{on } \Gamma, \quad \boldsymbol{\lambda}^{n+4/5} \in \Lambda_h^{n+4/5},\ \ \mathbf{V}^{n+1} \in \mathbb{R}^3,\ \ \boldsymbol{\omega}^{n+1} \in \mathbb{R}^3, \tag{43}$$

$$\langle \boldsymbol{\mu}, \mathbf{u}^{n+1} - \mathbf{V}^{n+1} - \boldsymbol{\omega}^{n+1} \times \overrightarrow{\mathbf{G}_j^{n+4/5}\mathbf{x}} \rangle_h = 0 \quad \forall \boldsymbol{\mu} \in \Lambda_h^{n+4/5}. \tag{44}$$

In (34)–(44), $\Gamma_-^{n+1} = \{\mathbf{x} \mid \mathbf{x} \in \Gamma,\ \mathbf{g}_{0h}^{n+1}(\mathbf{x}) \cdot \mathbf{n}(\mathbf{x}) < 0\}$ and $\mathbf{W}_{0h}^{n+1,-} = \{\mathbf{v} \mid \mathbf{v} \in \mathbf{W}_h, \mathbf{v} = 0 \text{ on } \Gamma_-^{n+1}\}$, $\Lambda_h^{n+s} = \Lambda_h(t^{n+s})$, and $\alpha + \beta = 1$. But in the numerical simulation, we usually choose $\alpha = 1$ and $\beta = 0$.

3.2. On the solution of subproblems (35), (36), (37), (38)–(42), and (43)–(44)

The degenerated quasi-Stokes problem (35) is solved by an Uzawa/preconditioned conjugate gradient algorithm as in [11], where the discrete elliptic problems from the preconditioning are solved

by a matrix-free fast solver from FISHPAK due to Adams et al. [1]. The advection problem (36) for the velocity field is solved by a wave-like equation method as in [4,5]. Problem (37) is a classical discrete elliptic problem which can be solved by the same matrix-free fast solver.

System (38)–(42) is a system of ordinary differential equations thanks to operator splitting. For its solution one can choose a time step smaller than Δt (i.e., we can divide Δt into smaller steps) to predict the translation velocity of the center of mass, the angular velocity of the particle, the position of the center of mass and the regions occupied by each particle so that the repulsion forces can be effective to prevent particle–particle and particle-wall overlapping. At each subcycling time step, keeping the distance as constant between the pair of points $\mathbf{x}_1$ and $\mathbf{x}_2$ in each particle is important since we are dealing with rigid particles. We have applied the following approach to satisfy the above constraint.

- Translate $\mathbf{x}_1$ and $\mathbf{x}_2$ according to the new position of the mass center at each subcyling time step.
- Rotate $\mathbf{G}\mathbf{x}_1$ and $\mathbf{G}\mathbf{x}_2$, the relative positions of $\mathbf{x}_1$ and $\mathbf{x}_2$ to the center of mass $\mathbf{G}$, by the following Crank–Nicolson scheme (a Runge–Kutta scheme of order 2 in fact):

$$\frac{\mathbf{G}\mathbf{x}_i^{\text{new}} - \mathbf{G}\mathbf{x}_i^{\text{old}}}{\tau} = \boldsymbol{\omega} \times \frac{\mathbf{G}\mathbf{x}_i^{\text{new}} + \mathbf{G}\mathbf{x}_i^{\text{old}}}{2} \tag{45}$$

for $i = 1, 2$ with τ as a subcyling time step. By (45), we have $|\mathbf{G}\mathbf{x}_i^{\text{new}}|^2 = |\mathbf{G}\mathbf{x}_i^{\text{old}}|^2$ for $i = 1, 2$ and $|\mathbf{G}\mathbf{x}_2^{\text{new}} - \mathbf{G}\mathbf{x}_1^{\text{new}}|^2 = |\mathbf{G}\mathbf{x}_2^{\text{old}} - \mathbf{G}\mathbf{x}_1^{\text{old}}|^2$ (i.e., scheme (45) is distance and in fact shape preserving).

After solving (38)–(42), the rigid-body motion is enforced in $B(t^{n+4/5})$, via Eq. (44). At the same time those hydrodynamical forces acting on the particles are also taken into account in order to update the translation and angular velocities of the particles. To solve (43)–(44), we use a conjugate gradient algorithm as discussed in [8]. Since we take $\beta = 0$ in (43) for the simulation, we actually do not need to solve any nontrivial linear systems for the velocity field; this saves a lot of computing time. To get the angular velocity $\boldsymbol{\omega}^{n+1}$, computed via

$$\boldsymbol{\omega}^{n+1} = (\mathbf{I}_{\text{p}}^{n+4/5})^{-1}(\mathbf{I}_{\text{p}}\boldsymbol{\omega})^{n+1}, \tag{46}$$

we need to have $\mathbf{I}_{\text{p}}^{n+4/5}$, the inertia of the particle $B(t^{n+4/5})$. We first compute the inertia $\mathbf{I}_0$ in the coordinate system attached to the particle. Then via the center of mass $\mathbf{G}^{n+4/5}$ and points $\mathbf{x}_1^{n+4/5}$ and $\mathbf{x}_2^{n+4/5}$, we have the rotation transformation $\mathbf{Q}$ ($\mathbf{Q}\mathbf{Q}^{\text{T}} = \mathbf{Q}^{\text{T}}\mathbf{Q} = \mathbf{I}_d$, $\det \mathbf{Q} = 1$) which transforms vectors expressed in the particle frame to vectors in the flow domain coordinate system and $\mathbf{I}_{\text{p}}^{n+s} = \mathbf{Q}\mathbf{I}_0\mathbf{Q}^{\text{T}}$. Actually in order to update matrix $\mathbf{Q}$, we can also use *quaternion* techniques, as shown, in the review paper [3].

4. Numerical experiments

In the test cases, we consider the simulation of the motion of a settling ellipsoid in a narrow channel of infinity length filled with a Newtonian fluid. The computational domain in $\Omega = (0, 1) \times (0, 0.25) \times (0.4)$ initially, then it moves down with the center of the ellipsoid (see, e.g., [13] for adjusting the computational domain according to the position of the particle). The fluid density is $\rho_{\text{f}} = 1$ and the fluid viscosity is $v_{\text{f}} = 0.01$. The flow field initial condition is $\mathbf{u} = \mathbf{0}$. The three semi-axes of the ellipsoid are 0.2, 0.1 and 0.1. The initial velocity and angular velocity of the ellipsoid are $\mathbf{0}$.

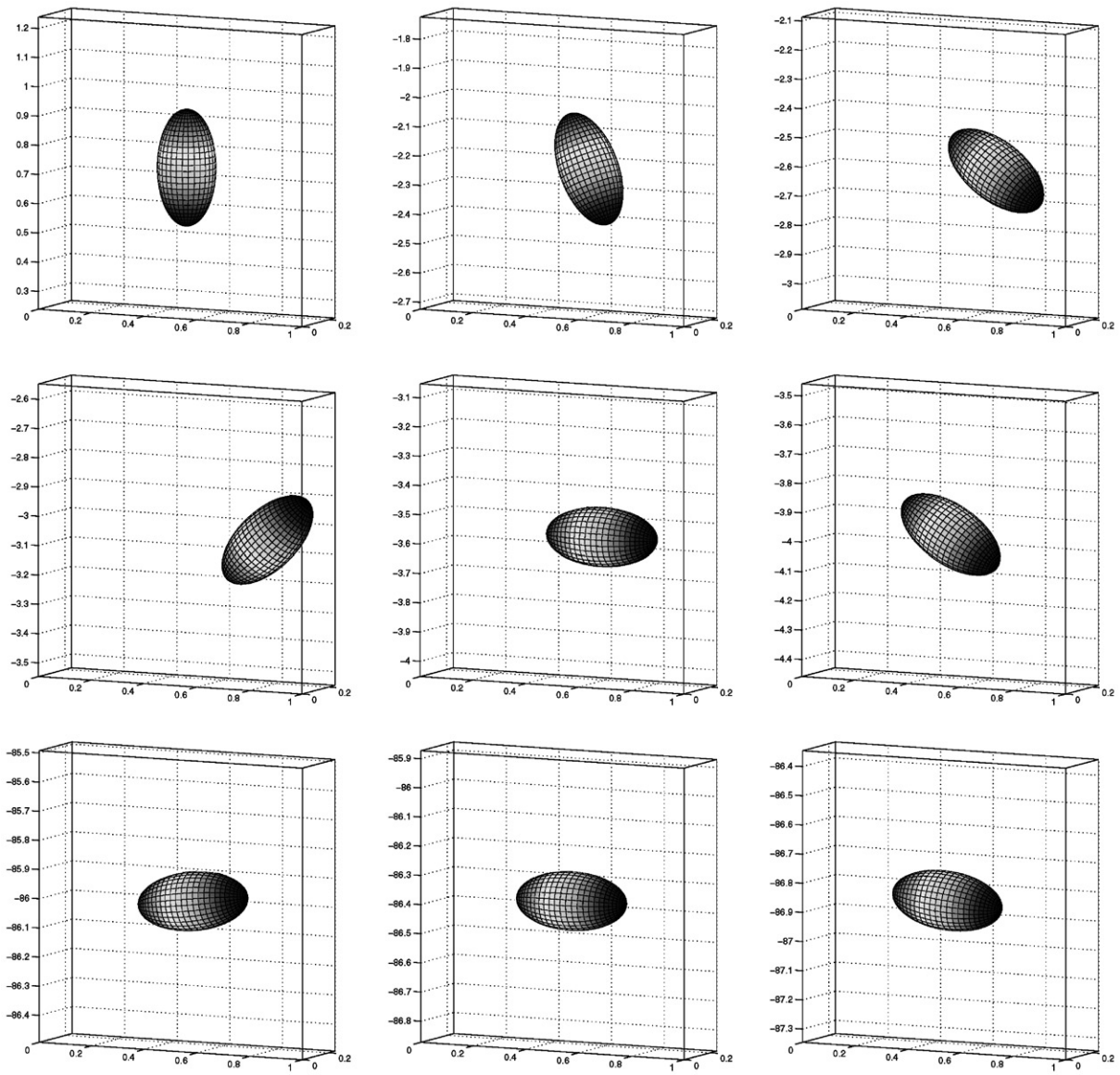

Fig. 2. Position of the ellipsoid at $t = 0$, 0.41, 0.46, 0.56, 0.66, 0.75, 18.1, 18.18, and 18.28 (from left to right and from top to bottom). The density of the ellipsoid is $\rho_s = 1.25$.

In the first case, the density of the ellipsoid is $\rho_s = 1.25$. Its vertical axis is the longest semi-axis (see Fig. 2). The mesh size for the velocity field (resp., pressure) is $h_v = 1/80$ (resp., $h_p = 2h_v$). The time step is $\Delta t = 0.001$. In Fig. 2, the positions of the ellipsoid at different times in the channel are shown. The motion of the ellipsoid is very violent at the beginning, it moves very close to the side wall after release from its initial position (see Fig. 2). Later on the motion becomes periodic (see Figs. 2 and 3). As expected, the ellipsoid turns its broadside to the stream while oscillating as

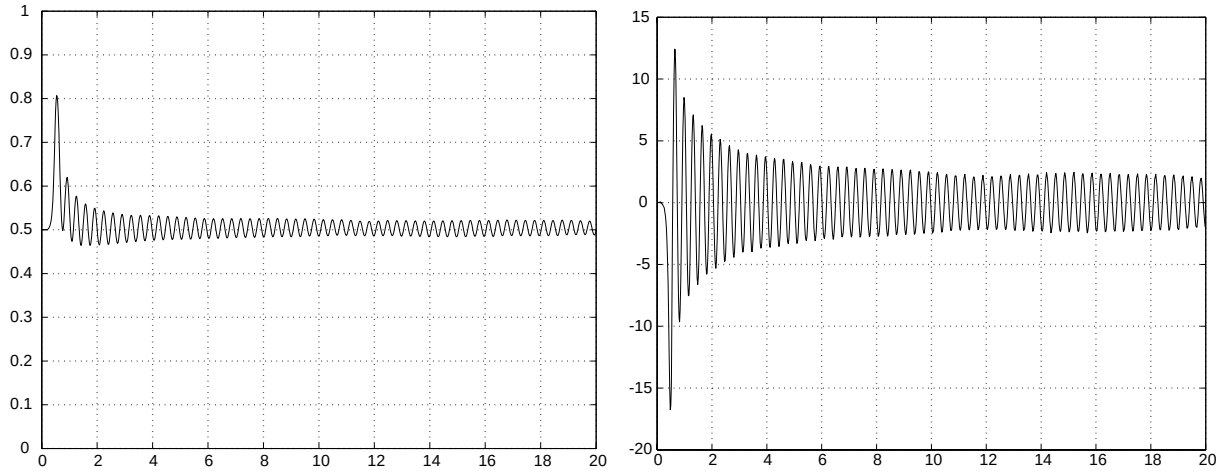

Fig. 3. Histories of the x-coordinate of the center (left) and the y-component of the angular velocity (right) of the ellipsoid of the density $\rho_s = 1.25$.

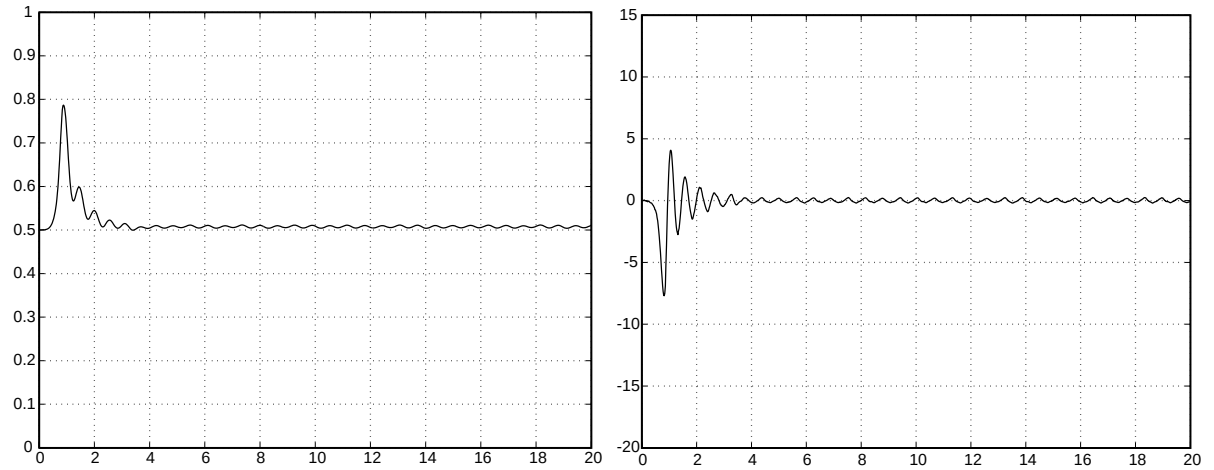

Fig. 4. Histories of the x-coordinate of the center (left) and the y-component of the angular velocity (right) of the ellipsoid of the density $\rho_s = 1.1$.

shown in the last three snapshots of Fig. 2. The averaged particle speed at the end of the simulation is about 4.256 so the particle Reynolds number with the long axis as characteristic length is 170.24. In the second case, the density of the ellipsoid is $\rho_s = 1.1$. The initial position is the same as the previous one. The mesh size for the velocity field (resp., pressure) is $h_v = 1/64$ (resp., $h_p = 2h_v$). The time step is $\Delta t = 0.001$. The averaged particle speed at the end of simulation is about 2.246. The angular velocity with respect to the y-axis is relative small compared to the one in the previous case (see Fig. 4) and the ellipsoid turns its broadside to the stream and oscillates much less.

Acknowledgements

We acknowledge the helpful comments and suggestions of E.J. Dean, J. He, H.H. Hu, P.Y. Huang, D.D. Joseph, Y. Kuznetsov and J. Periaux. We acknowledge also the support of NSF (grants ECS-9527123, CTS-9873236, DMS-9973318, and CCR-9902035), Texas Board of Higher Education (ARP grant 003652-0383-1999), and DOE/LASCI (grant R71700K-292-000-99).

References

[1] J. Adams, P. Swarztrauber, R. Sweet, FISHPAK: a package of Fortran subprograms for the solution of separable elliptic partial differential equations, The National Center for Atmospheric Research, Boulder, CO, 1980.
[2] F.P.T. Baaijens, A fictitious domain/mortar element method for fluid-structure interaction, Internat. J. Numer. Methods Fluids 35 (2001) 743–761.
[3] J.C.K. Chou, Quaternion kinematic and dynamic differential equations, IEEE Trans. Robot. Automat. 8 (1992) 53–64.
[4] E.J. Dean, R. Glowinski, A wave equation approach to the numerical solution of the Navier–Stokes equations for incompressible viscous flow, C.R. Acad. Sci. Paris, Sér. 1 325 (1997) 783–791.
[5] E.J. Dean, R. Glowinski, T.-W. Pan, A wave equation approach to the numerical simulation of incompressible viscous fluid flow modeled by the Navier–Stokes equations, in: J.A. De Santo (Ed.), Mathematical and Numerical Aspects of Wave Propagation, SIAM, Philadelphia, PA, 1998, pp. 65–74.
[6] R. Glowinski, T. Hesla, D.D. Joseph, T.-W. Pan, J. Périaux, Distributed Lagrange multiplier methods for particulate flows, in: M.O. Bristeau, G. Etgen, W. Fitzgibbon, J.L. Lions, J. Périaux, M.F. Wheeler (Eds.), Computational Science for the 21st Century, Wiley, Chichester, UK, 1997, pp. 270–279.
[7] R. Glowinski, T.-W. Pan, T. Hesla, D.D. Joseph, J. Périaux, A fictitious domain method with distributed Lagrange multipliers for the numerical simulation of particulate flow, in: J. Mandel, C. Farhat, X.C. Cai (Eds.), Domain Decomposition Methods 10, American Mathematical Society, Providence, RI, 1998, pp. 121–137.
[8] R. Glowinksi, T.-W. Pan, T. Hesla, D.D. Joseph, A distributed Lagrange multiplier/fictitious method for flows around moving rigid bodies: application to particulate flows, Int. J. Multiphase Flow 25 (1999) 755–794.
[9] R. Glowinski, T.-W. Pan, T. Hesla, D.D Joseph, J. Périaux, A distributed Lagrange multiplier/fictitious domain method for flow around moving rigid bodies: application to particulate flow, Internat. J. Numer. Methods Fluids 30 (1999) 1043–1066.
[10] R. Glowinski, T.-W. Pan, T.I. Hesla, D.D. Joseph, J. Périaux, A fictitious domain approach to the direct numerical simulation of incompressible viscous flow past moving rigid bodies: application to particulate flow, J. Comput. Phys. 169 (2001) 363–426.
[11] R. Glowinski, T.W. Pan, J. Périaux, Distributed Lagrange multiplier methods for incompressible flow around moving rigid bodies, Comput. Methods Appl. Mech. Eng. 151 (1998) 181–194.
[12] H.H. Hu, Direct simulation of flows of solid–liquid mixtures, Int. J. Multiphase Flow 22 (1996) 335–352.
[13] H.H. Hu, D.D. Joseph, M.J. Crochet, Direct simulation of fluid particle motions, Theoret. Comput. Fluid Dynamics 3 (1992) 285–306.
[14] A. Johnson, T. Tezduyar, 3-D simulation of fluid-rigid body interactions with the number of rigid bodies reaching 100, Comput. Methods Appl. Mech. Eng. 145 (1997) 301–321.
[15] Y.J. Liu, D.D. Joseph, Sedimentation of particles in polymer solutions, J. Fluid Mech. 255 (1993) 565–595.
[16] G.I. Marchuk, Splitting and alternating direction methods, in: P.G. Ciarlet, J.L. Lions (Eds.), Handbook of Numerical Analysis, North-Holland, Amsterdam, 1990, pp. 197–462.
[17] B. Maury, R. Glowinski, Fluid-particle flow: a symmetric formulation, C.R. Acad. Sci. Paris, Sér. 1 324 (1997) 1079–1084.
[18] T.-W. Pan, D.D Joseph, R. Bai, R. Glowinski, V. Sarin, Fluidization of 1204 spheres: simulation and experiments, J. Fluid Mech. 451 (2002) 169–191.
[19] T.-W. Pan, D.D. Joseph, R. Glowinski, Modeling Rayleigh–Taylor instability of a sedimenting suspension of several thousand circular particles in a direct numerical simulation, J. Fluid Mech. 434 (2001) 23–37.
[20] C.S. Peskin, Numerical analysis of blood flow in the heart, J. Comput. Phys. 25 (1977) 220–252.

[21] C.S. Peskin, Lectures on Mathematical Aspects of Physiology, Lectures in Applied Mathematics, Vol. 19, 1981, pp. 69–107.
[22] C.S. Peskin, D.M. McQueen, Modeling prosthetic heart valves for numerical analysis of blood flow in the heart, J. Comput. Phys. 37 (1980) 113–132.
[23] G.J. Wagner, N. Moes, W.K. Liu, T. Belytschko, The extended finite element method for rigid particles in Stokes flow, Internat. J. Numer. Methods. Eng. 51 (2001) 293–313.